Full Length Article

On the importance of the structure in the catalytic reactivity of Au-based catalysts

Luc Jacobs[a,b,*,1], Bernhard von Boehn[b,1], Mathias Homann[b], Cédric Barroo[a,c], Thierry Visart de Bocarmé[a,c], Ronald Imbihl[b,*]

[a] *Chemical Physics of Materials and Catalysis, Université libre de Bruxelles, CP243 Brussels, Belgium*
[b] *Institut für Physikalische Chemie und Elektrochemie, Leibniz Universität Hannover, Hannover, Germany*
[c] *Center for Nonlinear Phenomena and Complex Systems (CENOLI), Université libre de Bruxelles, CP231 Brussels, Belgium*

ABSTRACT

Au-based materials are remarkably efficient catalysts in the domain of partial oxidation reactions. Nonetheless, questions remain about the physico-chemical phenomena involved at the molecular level. In this work, the catalytic properties of Au-Ag samples, in the form of ultrathin Ag layers on a Au(1 1 1) surface and Au-based model nanoparticles, have been investigated with different microscopy techniques. Using photoemission electron microscopy (PEEM), the exposure of a Au(1 1 1) single crystal doped with various amounts of Ag (0 to 3 monolayers) to O_2/H_2 and O_2/CH_3OH gas mixtures did not lead to any specific spatiotemporal pattern formation. In contrast, the use of curved nanoscopic Au and Au-8.8 at.% Ag tip-samples analysed by field emission microscopy (FEM) under similar experimental conditions indicates the presence of catalytic activity. The influence of the silver concentration and of the morphology on the reactivity is discussed. This work highlights the necessity of different experimental approaches aimed at bridging the materials gap often encountered between surface science studies and applied catalysis.

1. Introduction

Soon after the discovery of the outstanding catalytic properties of gold nanoparticles [1], it was shown that the addition of a second metal to Au improves the overall reactivity and may even eliminate the particle size related deactivation of Au catalysts [2]. The increased reactivity depends on the intrinsic reactivity of the second metal towards specific reactions [3], but also on synergistic effects between Au and the second metal, even if the latter is only present in residual amounts. The origin of the unique performance of Au-Ag catalysts for partial oxidation reactions is attributed to such synergetic effects [4–6]. Catalytically very active systems like self-supported nanoporous (np) Au-Ag foams contain 1–3 at.% of Ag. The role of Ag is to promote the dissociation of molecular oxygen, while the chemically less active Au matrix is needed to guide the selectivity of the chemical reaction [7,8]. These highly porous crystalline systems contain a large fraction of low coordinated surface atoms. The resulting catalytic activity originates from the sum of different contributions such as the catalyst structure [1], its chemical composition [9] and its 3D morphology, which controls the gas diffusion within the pores and around the ligaments [10,11].

In this work, we use model systems of reduced complexity to obtain a better understanding of the phenomena at the molecular scale. We study bimetallic single crystal surfaces and bimetallic field emitter tips. Field emitter tips mimic single catalytic particles or ligaments of nanoporous structures in terms of size and morphology. Flat terraces represented by single crystal surfaces can also be found in crystalline nanoporous systems [12].

In a first step, a silver decorated Au(1 1 1) surface is analysed by photoemission electron microscopy (PEEM) coupled with *in situ* quadrupole mass spectrometry (QMS). With this catalytic model system, it should be possible to extract the influence of silver atoms on the catalytic activity, since the undecorated Au(1 1 1) crystal is considered to be catalytically inactive under the low pressure conditions used in this work ($p < 10^{-3}$ mbar).

In a second step, sharp Au and Au-Ag alloy tips with a diameter of 30–50 nm, are analysed by field emission microscopy (FEM). With these experiments, the contribution of Ag to the catalytic activity and the influence of the sample morphology can be studied. PEEM and FEM

* Corresponding authors at: Chemical Physics of Materials and Catalysis, Université libre de Bruxelles, CP243 Brussels, Belgium (L. Jacobs). Institut für Physikalische Chemie und Elektrochemie, Leibniz Universität Hannover, Hannover, Germany (R. Imbihl).
E-mail addresses: lucjacob@ulb.ac.be (L. Jacobs), imbihl@pci.uni-hannover.de (R. Imbihl).
[1] These authors contributed equally to this work.

experiments are performed during catalytic $O_2 + H_2$ and $O_2 + CH_3OH$ reactions. Structure-reactivity relationships have already been derived from Au-8.8 at.% Ag field emitter tips during hydrogenation of N_2O at 300–320 K [13]. A similar approach is taken here.

2. Experimental methods

The experiments on single crystal surfaces were carried out in a UHV system equipped with PEEM, a cylindrical mirror analyser for Auger electron spectroscopy (AES), a four-grid low-energy electron diffraction optics (LEED), and a differentially pumped quadrupole mass spectrometry (QMS). The Au(1 1 1) single crystal surface (*MaTeck GmbH*) was prepared by repeated cycles of Ar^+ ion sputtering in normal incidence (conditions: 1000 eV, 30 min, 3 µA, 300 K) and annealing at 923 K for 60 min. Cleaning cycles were carried out until no impurities were observed in AES and the typical (22 × √3) herringbone reconstruction of the Au(1 1 1) [14] surface was observed in LEED. Ag was deposited at room temperature under UHV conditions, onto the Au (1 1 1) surface by electron beam evaporation of a high purity Ag rod (*MaTeck GmbH*). The Ag deposition rate calibration was carried out using AES spectroscopy. Between every experiment, prior to the deposition of a new Ag layer, the Au(1 1 1) surface was cleaned by Ar^+ ion sputtering (500 eV, 10 min, 3 µA, 300 K) and annealing (923 K, 30 min) ensuring an identical starting point for every experiment.

The deposition rate calibration of Ag is shown in Fig. 1. The ratios between the Ag (350 eV) and Au (65, 140 and 239 eV) Auger peak intensities are plotted as a function of the deposition time. A linear increase is observed up to about 10 min, followed by a change in the slope which indicates the completion of the first Ag monolayer (ML). Such behaviour is typical of a layer by layer growth [15,16]. From the calibration curve, a deposition rate of 0.1 ML/min is obtained.

PEEM experiments and reaction rate measurements were carried out in the 10^{-4} mbar range and at temperatures ranging from 300 to 458 K. A deuterium discharge lamp (5–6.5 eV) was used to eject photoelectrons from the Au(1 1 1) surface. Consequently, changes in the photoemission current, seen as brightness variations on the detector screen, can be related to work function changes of the metal surface and hence, to changes in the chemical composition of the adsorbate layer [13]. For reaction rate measurements, the sample was placed in front of an extractor cone (6 mm opening diameter) leading to a differentially pumped QMS. With this continuous flow reactor set up, it is ensured

that all detected molecules have interacted with the surface of the specimen prior to detection. For technical reasons, QMS and PEEM measurements were not carried out simultaneously, but successively under the same experimental conditions.

Similar to PEEM measurements, FEM experiments rely on work function changes of metallic surfaces [17]. However, in FEM, the electron emission is triggered by the presence of an electric field of a few V·nm^{-1} between the specimen and the imaging screen. To induce sufficiently high electric fields without the need of high electric potentials, the samples were prepared as sharp tips: starting from a 0.1 mm alloy wire (*American Elements*, Au-8.8 at.% Ag) and from a 0.1 mm Au wire (*Advent Research Materials Ltd.*, purity 99.99%), the samples were shaped into their final form by electrochemical etching using the micro-electropolishing method in KCN solution (20 wt%, 4–7 V_{DC}) [13]. In this way, samples with a radius of 30–50 nm radius at the apex were obtained. *In situ* field evaporation steps allow to smoothen the surface and to reach a quasi-hemispherical shape. By applying a constant electric voltage (and hence electric field) and constant temperature, changes in brightness can be attributed to chemical variations of the adsorbate layer or to surface reconstructions, which can be imaged by field ion microscopy (FIM). FEM experiments were carried out in reactive gas atmospheres between 3×10^{-5} and 1×10^{-4} mbar at 300–500 K. After every set of experiments, flash-heating to 700 K and field evaporation of the first atomic layers were applied to desorb residual adsorbates and recover a similar starting state. The catalytic properties were evaluated in terms of brightness variations and QMS measurements for PEEM experiments, and brightness variations for FEM experiments. We mention that in all experiments, the pressure corresponds to the direct pressure read on Bayard-Alpert ionization gauges, sensitivity factors have not been taken into account (uncorrected pressures).

3. Results

3.1. Structural characterisations

The deposition of 1.6 ML Ag on the clean Au(1 1 1) surface results in a lifting of the (22 × √3) reconstruction and only the integer diffraction spots remain in LEED (not shown). No adsorbate superstructures are found in LEED in the presence of H_2, O_2 or CH_3OH (up to a pressure of 1×10^{-7} mbar at room temperature), neither on Au(1 1 1), nor on the
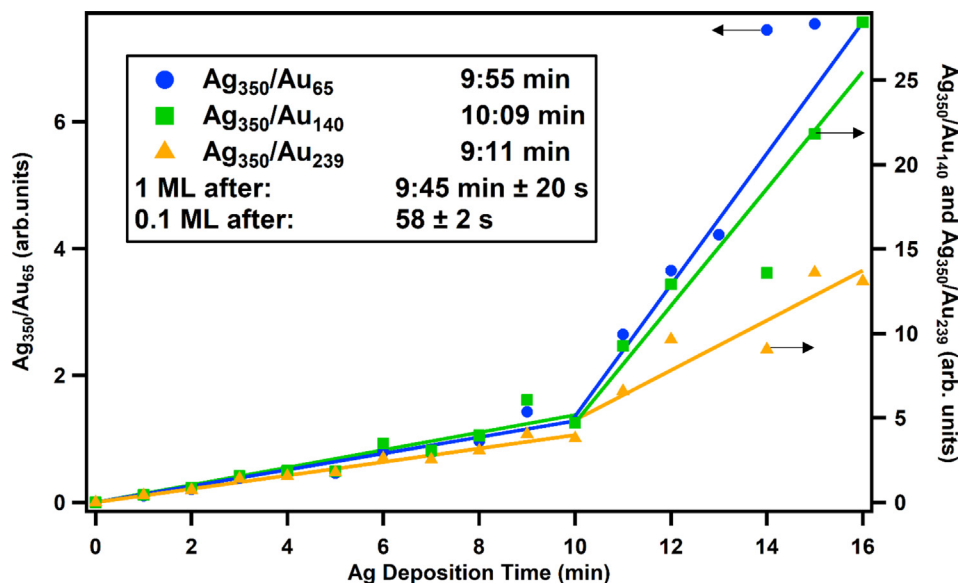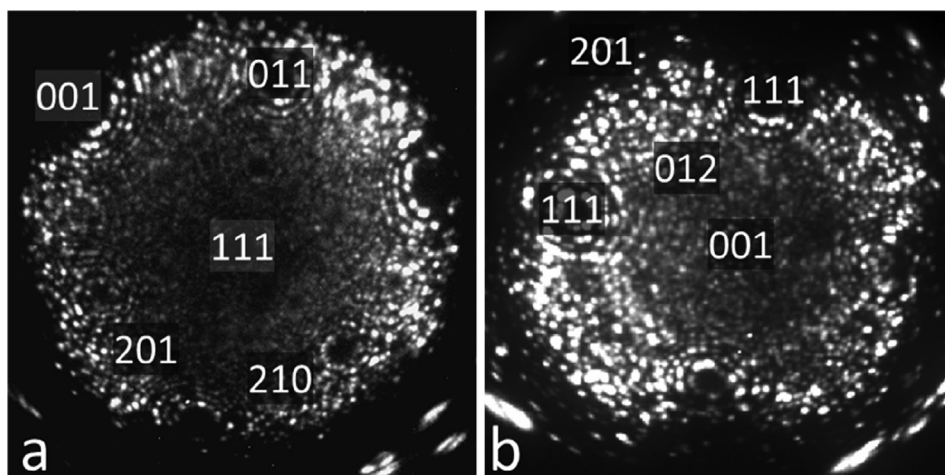

Fig. 1. Evolution of several Auger transitions during room temperature deposition of Ag onto Au(1 1 1). The calibration curves show different Ag/Au AES intensity ratios. The change in the slope after approximately 10 min of deposition time marks the completion of the first Ag monolayer.

Fig. 2. (a) Field ion micrograph of a clean Au-8.8 at.% Ag field emitter tip recorded under hydrogen atmosphere (imaging conditions: p (H_2) = 1.8 × 10^{-5} mbar, T = 60 K, F = 22 V·nm^{-1}) (b) Field ion micrograph of a clean Au field emitter tip (imaging conditions: p (H_2) = 1.5 × 10^{-5} mbar, T = 60 K, F = 22 V·nm^{-1}). The main crystallographic orientations are indicated by their Miller indices.

Ag covered Au(1 1 1) surface.

The structure of the field emitter tips was analysed by FIM micrographs with atomic resolution, as can be seen in Fig. 2a–b. It is possible to attribute Miller indices to the different visible crystallographic planes. This is important to assess the difference in reactivity detected during subsequent FEM experiments, and to assign them to the crystallographic orientation of the underlying facets. Furthermore, it is possible to detect surface reconstructions by comparing micrographs before and after reaction conditions were applied. Exposure to reactive gas atmospheres (H_2, O_2 and CH_3OH alone, and the mixtures (equal pressure readout of the constituents) from 3 × 10^{-5} to 1 × 10^{-4} mbar at temperatures from 300 to 500 K), as well as heating up to 700 K in vacuum (p < 1 × 10^{-9} mbar), did not induce any surface reconstructions. This indicates that the observed brightness variations in FEM are caused by chemical changes in the adsorbate layer and are not related to surface reconstructions.

3.2. Segregation of Ag

Silver species on gold surfaces are laterally mobile, but vertical diffusion into subsurface sites can also occur [18]. Consequently, the equilibrium surface composition is subject to the experimental parameters such as the initial distribution of silver, the gas phase composition, the pressure and the temperature. The dissolution of a 3 ML Ag film deposited at room temperature in the Au bulk was followed with AES during heating of the sample. The Au(1 1 1) surface covered with 3 ML of Ag was heated from 300 K to 673 K in 50 K steps (Fig. 3), while recording an AES spectrum at each step. As demonstrated in Fig. 3, the Ag 350 eV signal initially slightly increases to reach a maximum at 373 K, beyond which the signal decreases until it completely vanishes at 673 K. The initial increase is most likely due to thermal desorption of adsorbates which accumulated due to adsorption from the residual gas. At higher temperature, the decrease in signal intensity is caused by thermally-induced diffusion of Ag into the Au bulk. The onset of bulk diffusion is located between 473 and 523 K.

A temperature below 460 K is accordingly selected for the rate measurements in order to prevent thermally-induced diffusion of Ag into the Au bulk. Moreover, it was previously demonstrated by atom probe tomography that this temperature range does not induce any surface segregation of silver in Au-Ag alloy field emitter samples, in which Ag is homogeneously distributed [18]. Since Au-based catalysts are already active at relatively low temperature, 300–458 K is a convenient temperature range for catalytic measurements [6–8,19].

3.3. Catalytic properties

With PEEM, a series of experiments was carried out using different silver coverages ranging from θ_{Ag} = 0–3 ML. Experiments were carried out in pure H_2, O_2 or CH_3OH, and in 1:1 mixtures of O_2 + H_2 and O_2 + CH_3OH. The reactions were studied up to a total pressure of 1 × 10^{-4} mbar either at constant temperature (300, 373 and 458 K), or during linear heating ramps (0.5 K/s). No significant brightness variations or pattern formation were observed in PEEM in the parameter range. Increasing amounts of silver are supposed to enhance the O_2 splitting and should therefore result in an increased reactivity [20]. However, even after increasing the Ag coverage up to 3 ML, no significant brightness decreases were observed in PEEM upon exposure to pure oxygen, as well as to O_2 + H_2 and O_2 + CH_3OH mixtures.

Complementary QMS measurements were performed during the O_2 + H_2 and O_2 + CH_3OH reactions under the same experimental conditions. The low activity of the Au(1 1 1) and Ag/Au(1 1 1) surfaces observed in PEEM is reflected in the rate measurements, since product formation above the background noise level can hardly be detected.

Field emitter tips expose a large number of facets with different crystallographic orientations containing low coordinated surface atoms. Experiments are carried out using homogeneous Ag-Au alloy tips of Au-8.8 at.% Ag composition, and, for comparison, on pure Au tips. The homogeneous composition of these samples at the nanoscale has previously been confirmed by atom probe tomography [18]. Using pure Au tip-samples, introducing H_2, O_2 or CH_3OH, as well as the corresponding mixtures (O_2 + H_2 and O_2 + CH_3OH, 1:1 ratio of partial pressures at p = 3 × 10^{-5} mbar) at 300 and 400 K does not produce any significant intensity variations above the background noise level. The same experiments are conducted on Au-8.8 at.% Ag samples in which cases, for all applied experimental conditions, strong brightness variations are recorded, as can be seen in representative snapshots obtained during FEM experiments on an Au-8.8 at.% Ag sample. Fig. 4 displays snapshots recorded during the O_2 + H_2 reaction at 400 K. At constant electric field (estimated intensity between 4 and 6 V·nm^{-1}, based on the radius of the tip and the applied voltage), and at constant pressure and temperature. Since no reconstruction occurred, a change in the emission pattern indicates a change in the chemical composition of the adsorbate layer. Qualitatively, in our system, a darker emission pattern is a sign of an oxygen-covered surface as O(ads) is known to increase the work function of both gold ($\Delta\varphi \approx$ 1 eV [21]) and silver surfaces ($\Delta\varphi \approx$ 0.6–0.8 eV [22]). An increased brightness indicates water formation as adsorbed water molecules decrease the work function of both gold and silver surfaces [23]. Furthermore, the desorption of water from the surface generates vacant sites: the combination of water formation and desorption is translated into an increase of brightness as compared to an oxygen-covered surface. The emission of electrons from the specimen depends on the crystallographic orientation of the facets, and the field emission pattern can be seen as a two-dimensional map of the work function along the surface of the tip apex. During our
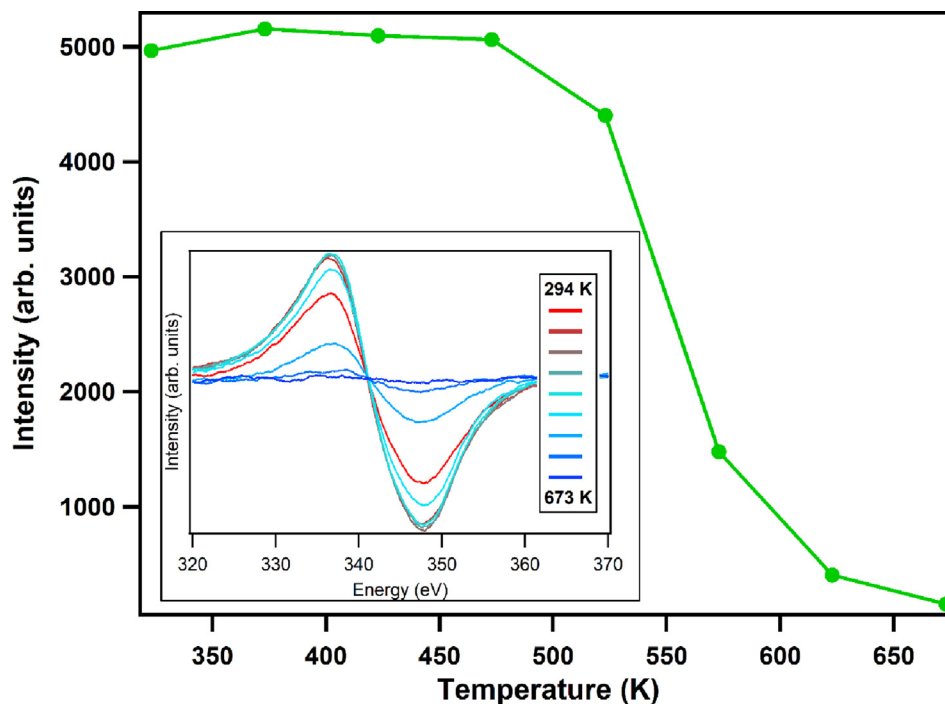
Fig. 3. Evolution of the 350 eV Ag AES peak intensity during step-wise heating of an Au(1 1 1) single crystal covered with 3 ML Ag. The diffusion of Ag into the Au bulk starts at 473–523 K.

experiments, we can observe that the overall emission intensity oscillates irregularly (Fig. 5). The brightness variations indicate that the surface composition changes from O-covered (dark – Fig. 4a and c) to O-free via H_2O formation (bright – Fig. 4b and d) in a random fashion. The more open facets of {0 1 2} orientation are the brightest at any

stage of the experiment. The integral intensity variations are a sign of chemical changes of the surface occurring homogeneously over the whole probed area (red circle – Fig. 4b). It has to be noted that although brightness variations occur over the whole surface, the largest intensity variations are observed on the {0 1 2} facets. This finding suggests that

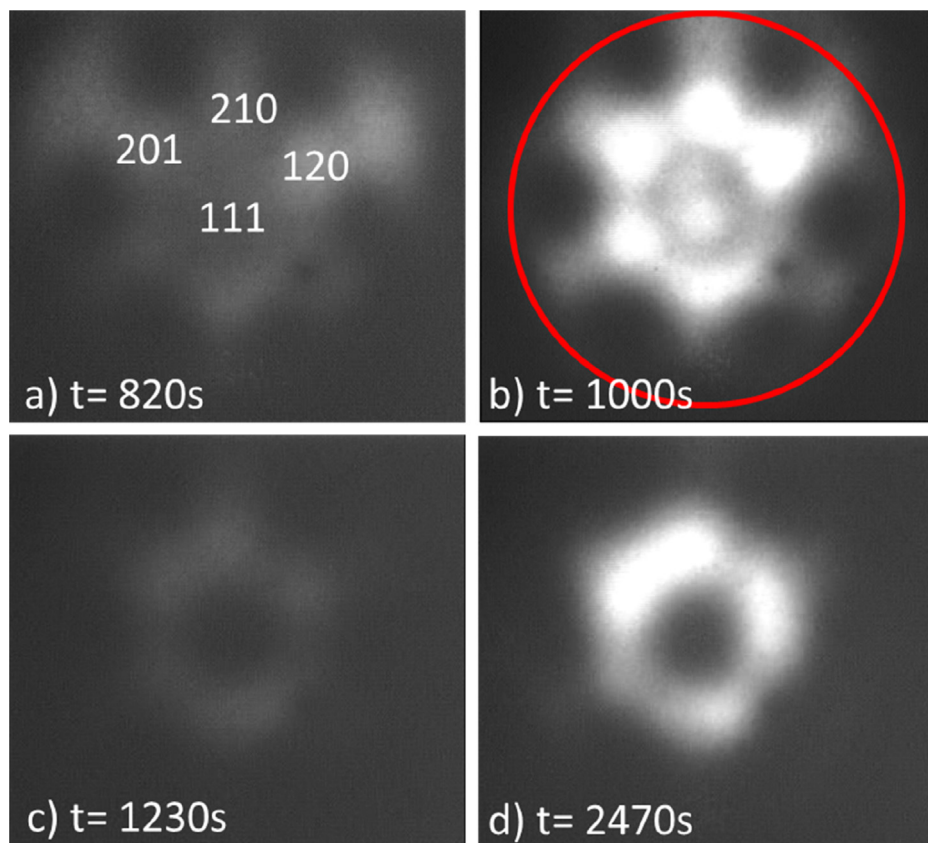**Fig. 4.** FEM images recorded during the $O_2 + H_2$ reaction over an Au-8.8 at.% Ag tip-sample illustrating the brightness variations due to the presence of a catalytic reaction, $T = 400$ K, $p(H_2) = p$ $(O_2) = 1.5 \times 10^{-5}$ mbar. The radius of the tip is estimated to be 15–20 nm. Red circle (a): Region of interest probed for the brightness analysis shown in Fig. 5. (For interpretation of the references to colour in this figure legend, the reader is referred to the web version of this article.)
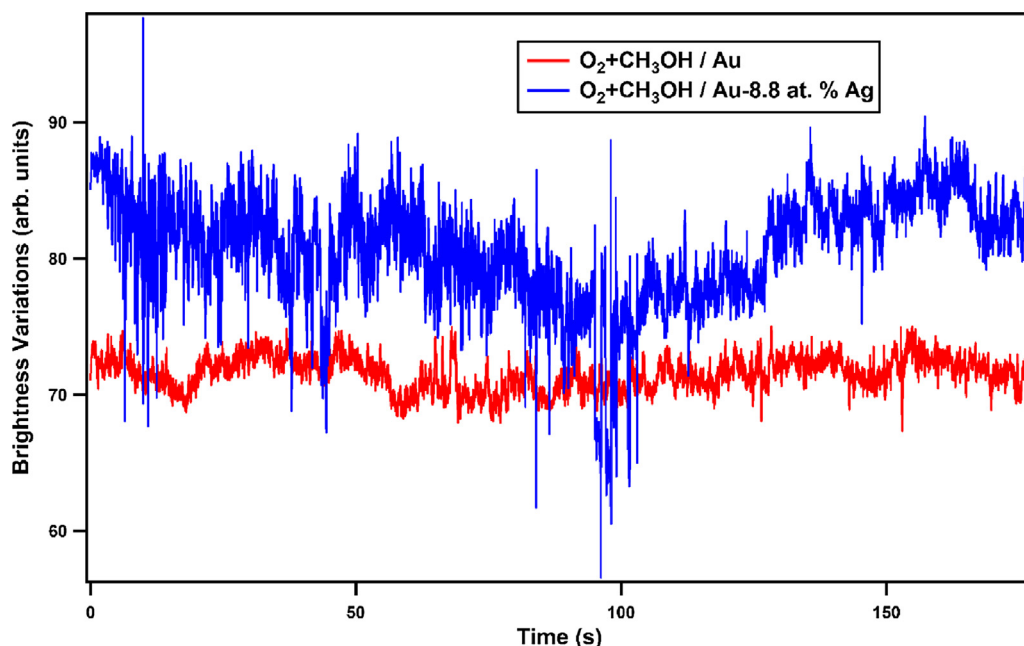
Fig. 5. Brightness variations recorded in FEM over Au and Au-8.8 at.% Ag field emitter tips in the presence of an O_2 + CH_3OH mixture (equal pressure readout, p_{tot} = 3 × 10^{-5} mbar) at 400 K, demonstrating the difference in catalytic activity of Au and Ag-Au tips. The brightness is probed over the whole visible field emission pattern, as indicated by the red circle in Fig. 4b, averaging the signals from both active and non-active facets. (For interpretation of the references to colour in this figure legend, the reader is referred to the web version of this article.)

the highest intrinsic activity is found on these facets, which is in line with a previous study where it was discovered that both, the adsorption and dissociation of N_2O, are regiospecific and limited to the {0 1 2} facets [13]. However, in the frame of this work, clear signs of reactivity are present on other facets too, suggesting a different structure–-reactivity relationship apparently due to the different nature of the oxidizing gas.

Similar observations are made during the O_2 + CH_3OH reaction. To illustrate the influence of Ag on the reactivity, Fig. 5 shows the brightness signal recorded in an oxygen and methanol gas mixture on pure Au and Au-8.8 at.% Ag at 400 K. The time constants of the variations range from seconds to minutes. In this plot, the brightness represents the overall intensity, averaged over the whole visible region in FEM, incorporating all facets present at the apex of the sample. An example of the probed region is shown with the red circle in Fig. 4.b. With the presence of active and inactive facets, the brightness variations are averaged, and locally important variations are lessened.

Whereas on pure Au intensity excursions are comprised within the fluctuation amplitudes inherent to the imaging of nanoscale systems, the presence of Ag in Au-8.8 at.% Ag specimen leads to stronger variations of the brightness signal, clearly indicating the occurrence of adsorption/desorption phenomena and/or surface reactions under identical experimental conditions. By analysing separate crystallographic planes, i.e. dense facets ({1 1 1} and {1 1 3}) and open facets ({0 1 1} and {0 1 2}), we observe that the brightness variations qualitatively follow a similar trend: the variations are roughly 50% larger in amplitude on the open facets as compared to the close-packed facets. This indicates a higher reactivity of the more open facets.

Chemically, the oxidation of methanol proceeds inhomogeneously over the tip-sample since the oxidation rate depends on the oxygen coverage of the catalytic surface, and hence on the concentration of silver. Indeed, even though the initial composition of the sample is homogeneous, the O_2 adsorption and dissociation energies vary from one facet to another, which may lead to a non-homogeneous concentration of Ag in the very first surface layers [13]. The pronounced and rapid brightness variations observed on the Au-Ag alloy tip indicate that the adsorbate composition changes rapidly between reaction intermediates, which increase the work function (O(ads) [21,22]), and a state of the surface with lower work function, e.g. CH_3O(ads) [24]) and an adsorbate-free surface. FEM imaging, however, does not allow to chemically probe the composition of the adsorbate layer, and 1D atom

probe experiments are required to reveal the adsorbate composition.

3.4. Discussion

Using PEEM, during both, the O_2 + H_2 and the O_2 + CH_3OH reactions, no significant brightness variations were observed on Au(1 1 1) and Ag/Au(1 1 1). This indicates that, within the detection limits, no catalytic reaction and no adsorption of molecules took place. On pure Au(1 1 1) and up to 500 K, the sticking coefficient of O_2 is known to be extremely low, in such a way that chemisorption is not detectable [25–27]. One could expect an improved reactivity following Ag deposition, since Ag is known to facilitate dissociative O_2 adsorption [28]. As Au and Ag have similar lattice parameters (Au = 408 pm, Ag = 409 pm), deposited Ag layers grow epitaxially on Au(1 1 1), as confirmed by LEED showing a clear (1 × 1) diffraction pattern after Ag deposition. Apparently, this epitaxially grown Ag layer is catalytically quite inactive. Since the dissociative sticking coefficients for O_2 on Ag (1 1 1) lies in the 10^{-6} range for temperatures between 150 and 490 K [29,30], only a very minor increase in reactivity can be expected, which is in agreement with our observations.

To assess the effect of the structure on the reactivity, we used a similar approach with tip-samples in FEM. In the case of the O_2 + H_2 reaction, the use of pure Au specimens reveals a very low catalytic activity, as in the case of pure Au(1 1 1) using PEEM. Au nanoparticles are known to be catalytically active, but the low activity of the Au tips can be explained by the size-dependence of the reactivity of Au nanoparticles. The apex diameter of more than 30 nm of the Au tips is nearly one order of magnitude higher than the critical size required for Au nanoparticles to be active in O_2 dissociation [31].

Interestingly, on the Au-Ag alloy samples, clear signs of reactivity were observed in FEM. In the case of Au-8.8 at.% Ag specimens, the role of Ag in the catalytic performance is clearly identifiable. Ag sites promote the dissociation of O_2, leading to the formation of O(ads) species. This species increases the work function, as shown in Fig. 4. The oxygen covered surface is reacted-off to water via dissociative chemisorption of H_2, followed by reaction of the atomic adsorbates. During this reaction, a brighter emission pattern is observed which is due to both the formation of water known to decrease the work function of Au and Ag surfaces [23,32], and the subsequent formation of vacant sites.

Similar bright/dark changes are observed in the O_2 + CH_3OH reaction at 400 K over Au-8.8 at.% Ag samples. A bright area could

indicate the adsorption of methanol at the surface of the catalyst, presumably in the form of methoxy groups [24]. Alternatively, the presence of OH groups, of adsorbed water molecules or of other C-containing species should be taken into account. In order to clarify the chemical nature of the adsorbates, further experiments on tip samples with pulsed field desorption mass spectrometry, also known as 1D atom probe [33], are planned. These experiments should allow to determine the exact composition of the adsorbate layer during reaction.

For the $H_2 + O_2$ and $CH_3OH + O_2$ reactions, the presence of Ag atoms on a Au surface apparently plays an important role for generating catalytic reactivity. Based on pre-characterisation of the tips by FIM and assignment of the crystallographic orientations of the different facets, the reactions seem to take place over the whole imaged surface, with variations in the local reactivities depending on the crystallographic orientations of the exposed facets. This suggests that both, the presence of Ag and the presence of low-coordinated atoms (found at the steps, kinks and at the intersection between different facets on a model tip) promote reactivity. This is the key observation of this study.

In order to evaluate the relevance of the results obtained in our PEEM/QMS (300–458 K) and FEM (300–500 K) low pressure experiments, as compared to studies carried out at higher pressures, the conversion, selectivity and reaction mechanisms obtained in both cases should be compared. However, the small brightness variations observed in PEEM and the low amount of detected products in QMS do not allow to derive such information. In FEM, the composition of the adsorbate layer during brightness variations was discussed from a qualitative point of view, profiting from the distinctive effects that different reactants, reaction intermediates or products may have on the work function of the sample. In this way we proposed the presence of different species, like adsorbed methoxy groups. Even if it is not possible to determine the selectivity or propose a complete reaction mechanism, our observations and propositions match previously reported results [34]. Pulsed field desorption mass spectrometry experiments will help to further develop these discussions. Nonetheless it became clear that in case of Au-based catalysts, the influence of the structure on the reactivity is as important as the influence of the chemical composition.

These above observations might raise questions about the validity of using Ag/Au(1 1 1) as a model system for Au-Ag catalysts. The use of field emitter tips and of single crystals allows, to some extent, to bridge the materials gap. The simplified models used in this work have proven to yield important results, especially regarding the question of the structural prerequisites needed for Au-Ag catalysts. Some carefulness is also required when comparing the results presented here with mass spectrometry data obtained by other groups [34,35]. The remarkable activity of Au(1 1 1) surfaces and the extraordinary selectivities reported by other groups are only achieved using specific methodologies (use of O_3 or electron beam dissociation of O_2) to pre-cover the single crystals used with O(ads) prior to exposure to a reactive environment. These results are certainly of great importance to understand nanoporous gold systems under working conditions, but they neglect, to a certain extent, the question about the influence of silver on the O_2 splitting properties under reduced pressure conditions on model surfaces without pre-treatment. These aspects have to be contrasted with the results of this work: that is the importance of low coordinated surface atoms and the presence of surface silver for the catalytic activity of Au-Ag catalysts in low pressure oxidation reactions with molecular oxygen as oxidising agent, therefore giving insights into the intrinsic properties of the catalyst towards O_2 dissociation and methanol oxidation.

4. Conclusions

Two *in situ* electron microscopy techniques, PEEM and FEM, were used to analyse the reactivity of Au and Au-Ag model catalysts and to assess the influence of the surface composition, structure and morphology on the reactivity during $O_2 + H_2$ and $O_2 + CH_3OH$ reactions.

A Au(1 1 1) single crystal surface covered with variable amounts of silver was used in PEEM and Au and Au-8.8 at.% Ag alloy tips were used in FEM. In both cases, the exposure to reactive gas mixtures at different temperatures did not lead to any surface reconstructions of the Au-Ag catalysts, ensuring that the brightness changes translate variations of the adsorbate layer composition. During experiments on pure Au systems, a low reactivity was observed in PEEM and FEM, mainly due to the low sticking coefficient and the size-dependence of the reactivity. The presence of up to three monolayers of Ag on Au(1 1 1) didn't lead to an increase of reactivity. However, Au-8.8 at.% Ag tips exhibit catalytic activity in the $O_2 + H_2$ and $O_2 + CH_3OH$ reactions, stressing the importance of both the presence of Ag and of low coordinated surface atoms in the emergence of reactivity.

As a general conclusion, the presence of Ag is a necessity to obtain catalytic activity in Au-based model catalysts, but it is not a sufficient criterium: the structure of the material is crucial. This highlights the importance of designing catalysts with suitable structure and morphology at the nanoscale.

CRediT authorship contribution statement

Luc Jacobs: Conceptualization, Data curation, Formal analysis, Funding acquisition, Investigation, Methodology, Validation, Visualization, Writing - original draft, Writing - review & editing. **Bernhard von Boehn:** . **Mathias Homann:** . **Cédric Barroo:** Conceptualization, Data curation, Formal analysis, Funding acquisition, Investigation, Methodology, Supervision, Visualization, Writing - original draft, Writing - review & editing. **Thierry Visart de Bocarmé:** Supervision, Writing - review & editing. **Ronald Imbihl:**.

Declaration of Competing Interest

The authors declare that they have no known competing financial interests or personal relationships that could have appeared to influence the work reported in this paper.

Acknowledgements

References

[1] E. Genty, L. Jacobs, T. Visart de Bocarmé, C. Barroo, Dynamic processes on gold-based catalysts followed by environmental microscopies, Catalyst 7 (2017) 134.
[2] M. Haruta, Size- and support-dependency in the catalysis of gold, Catal. Today. 36 (1997) 153–166.
[3] J.L.C. Fajín, M.N.D.S. Cordeiro, J.R.B. Gomes, DFT study on the reaction of O_2 dissociation catalyzed by gold surfaces doped with transition metal atoms, Appl. Catal. A. 458 (2013) 90–102.
[4] G.J. Hutchings, Catalysis by gold: recent advances in oxidation reactions, in: B. Zhou, S. Han, R. Raja, G.A. Somorjai (Eds.), Nanotechnol. Catal. Springer, New York, 2007, pp. 39–51.
[5] A. Wittstock, V. Zielasek, J. Biener, C.M. Friend, M. Bäumer, Nanoporous gold catalysts for selective gas-phase oxidative coupling of methanol at low temperature, Science 327 (2010) 319–322.
[6] M.L. Personick, B. Zugic, M.M. Biener, J. Biener, R.J. Madix, C.M. Friend, Ozone-activated nanoporous gold: a stable and storable material for catalytic oxidation, ACS Catal. 5 (2015) 4237–4241.
[7] L. Wang, M.L. Personick, S. Karakalos, R. Fushimi, C.M. Friend, R.J. Madix, Active sites for methanol partial oxidation on nanoporous gold catalysts, J. Catal. 344 (2016) 778–783.
[8] B. Zugic, L. Wang, C. Heine, D.N. Zakharov, B.A.J. Lechner, E.A. Stach, J. Biener, M. Salmeron, R.J. Madix, C.M. Friend, Dynamic restructuring drives the catalytic activity on nanoporous gold – silver alloy catalysts, Nat. Mater. 16 (2016) 558–564.
[9] T. Juarez, J. Biener, J. Weissmüller, A.M. Hodge, Nanoporous metals with structural hierarchy: a review, Adv. Eng. Mater. 19 (2017) 1700389.

[10] G. Falcucci, S. Succi, A. Montessori, S. Melchionna, P. Prestininzi, C. Barroo, D.C. Bell, M.M. Biener, J. Biener, B. Zugic, E. Kaxiras, Mapping reactive flow patterns in monolithic nanoporous catalysts, Microfluid. Nanofluid. 20 (2016) 105.

[11] M.M. Montemore, A. Montessori, S. Succi, C. Barroo, G. Falcucci, D.C. Bell, E. Kaxiras, Effect of nanoscale flows on the surface structure of nanoporous catalysts, J. Chem. Phys. 146 (2017) 214703.

[12] T. Fujita, P. Guan, K. McKenna, X. Lang, A. Hirata, L. Zhang, T. Tokunaga, S. Arai, Y. Yamamoto, N. Tanaka, Y. Ishikawa, N. Asao, Y. Yamamoto, J. Erlebacher, M. Chen, Atomic origins of the high catalytic activity of nanoporous gold, Nat. Mater. 11 (2012) 775–780.

[13] L. Jacobs, C. Barroo, N. Gilis, S.V. Lambeets, E. Genty, T. Visart de Bocarmé, Structure reactivity relationships during N₂O hydrogenation over Au-Ag alloys: A study by field emission techniques, Appl. Surf. Sci. 435 (2018) 914–919.

[14] M.A. Van Hove, R.J. Koestner, P.C. Stair, J.P. Bibérian, L.L. Kesmodel, I. Bartoš, G.A. Somorjai, The surface reconstructions of the (100) crystal faces of iridium, platinum and gold, Surf. Sci. 103 (1981) 189–217.

[15] R.J. Culbertson, L.C. Feldman, P.J. Silverman, H. Boehm, Epitaxy of Au on Ag(111) studied by high-energy ion scattering, Phys. Rev. Lett. 47 (1981) 657–660.

[16] Y. Tanishiro, H. Kanamori, K. Takayanagi, K. Yagi, G. Honjo, UHV transmission electron microscopy on the reconstructed surface of (111) gold, Surf. Sci. 11 (1981) 395–413.

[17] G.V. Hansson, Photoemisison study of the bulk and surface electronic structure of single crystals of gold, Phys. Rev. B 18 (1978) 1572–1585.

[18] N. Gilis, L. Jacobs, C. Barroo, T. Visart de Bocarmé, Surface segregation in Au-Ag alloys investigated by atom probe tomography, Top. Catal. 61 (2018) 1437–1448.

[19] M. Haruta, T. Kobayashi, H. Sano, N. Yamada, Novel gold catalysts for the oxidation of carbon monoxide at a temperature far below 0°C, Chem. Lett. 16 (1987) 405–408.

[20] B. Zugic, L. Wang, C. Heine, D.N. Zakharov, B.A.J. Lechner, E.A. Stach, J. Biener, M. Salmeron, R.J. Madix, C.M. Friend, Dynamic restructuring drives catalytic activity on nanoporous gold-silver alloy catalysts, Nat. Mater. 16 (2017) 558–564.

[21] J.M. Gottfried, CO Oxidation over gold, PhD Thesis Freie Universität, Berlin, 2003.

[22] P. Wissmann, H.-U. Finzel, Electrical resistivity of thin metal films, Springer, Karlsruhe, 2007.

[23] R. Bryl, R. Blaszczyszyn, Surface diffusion of water on clean and Au-covered tungsten field emitter tips, Vacuum 54 (1999) 103–112.

[24] M. N'dollo, P.S. Moussounda, T. Dintzer, B. M'Passi-Mabiala, F. Garin, Density functional theory (DFT) investigation of the adsorption of the CH₃OH/Au(110) system, Surf. Interface Anal. 45 (2013) 1410–1418.

[25] J. Gong, C.B. Mullins, Surface science investigations of oxidative chemistry on gold, Acc. Chem. Res. 42 (2009) 1063–1073.

[26] A.G. Sault, R.J. Madix, C.T. Campbell, Adsorption of oxygen and hydrogen on Au (110)-(1x2), Surf. Sci. 169 (1986) 347–356.

[27] T. Visart de Bocarmé, T.-D. Chau, F. Tielens, J. Andrés, P. Gaspard, R.L.C. Wang, H.J. Kreuzer, N. Kruse, Oxygen adsorption on gold nanofacets and model clusters, J. Chem. Phys. 125 (2006) 054703.

[28] H.A. Engelhardt, D. Menzel, Adsorption of oxygen on silver crystal surfaces, Surf. Sci. 57 (1976) 591–618.

[29] C.T. Campbell, Atomic and molecular oxygen adsorption on Ag(111), Surf. Sci. 157 (1985) 43–60.

[30] C.T. Campbell, M.T. Paffett, The interactions of O₂, CO and CO₂ with Ag(110), Surf. Sci. 143 (1984) 517–535.

[31] M.-C. Daniel, D. Astruc, Gold nanoparticles: assembly, supramolecular chemistry, quantum-size-related properties, and applications toward biology, catalysis, and nanotechnology, Chem. Rev. 104 (2004) 293–346.

[32] R.L. Wells, T. Fort Jr., Adsorption of water on clean gold by measurement of work function changes, Surf. Sci. 32 (1972) 554–560.

[33] C. Barroo, M. Moors, T. Visart de Bocarmé, Imaging and chemically probing catalytic processes using field emission techniques: a study of NO hydrogenation on Pd and Pd-Au, Catal. Sci. Technol. 7 (2017) 5249–5256.

[34] L.-C. Wang, K.J. Stowers, B. Zugic, M.M. Biener, J. Biener, C.M. Friend, R.J. Madix, Methyl ester synthesis catalyzed by nanoporous gold: From 10⁻⁹ torr to 1 atm, Catal. Sci. Technol. 5 (2015) 1299–1306.

[35] C. Reece, E.A. Redekop, S. Karakalos, C.M. Friend, R.J. Madix, Crossing the great divide between single-crystal reactivity and actual catalyst selectivity with pressure transients, Nat. Catal. 1 (2018) 852–859.